5. Minami M, Daimon Y, Mori K, Takashima H, Nakajima T, Itoh Y, et al. Hepatitis B virus-related insertional mutagenesis in chronic hepatitis B patients as an early drastic genetic change leading to hepatocarcinogenesis. Oncogene 2005;24:4340-4348.
6. Kim CM, Koike K, Saito I, Miyamura T, Jay G. HBx gene of hepatitis B virus induces liver cancer in transgenic mice. Nature 1991;351:317-320.
7. Murakami S, Cheong JH, Kaneko S. Human hepatitis virus X gene encodes a regulatory domain that represses transactivation of X protein. J Biol Chem 1994;269:15118-15123.
8. Murakami S, Cheong J, Ohno S, Matsushima K, Kaneko S. Transactivation of human hepatitis B virus X protein, HBx, operates through a mechanism distinct from protein kinase C and okadaic acid activation pathways. Virology 1994;199:243-246.
9. Lin Y, Nomura T, Yamashita T, Dorjsuren D, Tang H, Murakami S. The transactivation and p53-interacting functions of hepatitis B virus X protein are mutually interfering but distinct. Cancer Res 1997;57:5137-5142.
10. Yasui K, Wakita T, Tsukiyama-Kohara K, Funahashi SI, Ichikawa M, Kajita T, et al. The native form and maturation process of hepatitis C virus core protein. J Virol 1998;72:6048-6055.
11. Hsieh TY, Matsumoto M, Chou HC, Schneider R, Hwang SB, Lee AS, et al. Hepatitis C virus core protein interacts with heterogeneous nuclear ribonucleoprotein K. J Biol Chem 1998;273:17651-17659.
12. Colombari R, Dhillon AP, Piazzola E, Tomezzoli AA, Angelini GP, Capra F, et al. Chronic hepatitis in multiple virus infection: histopathological evaluation. Histopathology 1993;22:319-325.
13. Honda M, Kaneko S, Kawai H, Shirota Y, Kobayashi K. Differential gene expression between chronic hepatitis B and C hepatic lesion. Gastroenterology 2001;120:955-966.
14. Desmet VJ, Gerber M, Hoofnagle JH, Manns M, Scheuer PJ. Classification of chronic hepatitis: diagnosis, grading and staging. HEPATOLOGY 1994;19:1513-1520.
15. Shirota Y, Kaneko S, Honda M, Kawai HF, Kobayashi K. Identification of differentially expressed genes in hepatocellular carcinoma with cDNA microarrays. HEPATOLOGY 2001;33:832-840.
16. Kawai HF, Kaneko S, Honda M, Shirota Y, Kobayashi K. Alpha-fetoprotein-producing hepatoma cell lines share common expression profiles of genes in various categories demonstrated by cDNA microarray analysis. HEPATOLOGY 2001;33:676-691.
17. Kawaguchi K, Honda M, Yamashita T, Shirota Y, Kaneko S. Differential gene alteration among hepatoma cell lines demonstrated by cDNA microarray-based comparative genomic hybridization. Biochem Biophys Res Commun 2005;329:370-380.
18. Honda M, Kawai H, Shirota Y, Yamashita T, Kaneko S. Differential gene expression profiles in stage I primary biliary cirrhosis. Am J Gastroenterol 2005;100:2019-2030.
19. Honda M, Kawai H, Shirota Y, Yamashita T, Takamura T, Kaneko S. cDNA microarray analysis of autoimmune hepatitis, primary biliary cirrhosis and consecutive disease manifestation. J Autoimmun 2005;25:133-140.
20. Yamashita T, Hashimoto S, Kaneko S, Nagai S, Toyoda N, Suzuki T, et al. Comprehensive gene expression profile of a normal human liver. Biochem Biophys Res Commun 2000;269:110-116.
21. Yamashita T, Kaneko S, Hashimoto S, Sato T, Nagai S, Toyoda N, et al. Serial analysis of gene expression in chronic hepatitis C and hepatocellular carcinoma. Biochem Biophys Res Commun 2001;282:647-654.
22. Mootha VK, Lindgren CM, Eriksson KF, Subramanian A, Sihag S, Lehar J, et al. PGC-1alpha-responsive genes involved in oxidative phosphorylation are coordinately downregulated in human diabetes. Nat Genet 2003; 34:267-273.
23. Watashi K, Ishii N, Hijikata M, Inoue D, Murata T, Miyanari Y, et al. Cyclophilin B is a functional regulator of hepatitis C virus RNA polymerase. Mol Cell 2005;19:111-122.
24. Nakagawa M, Sakamoto N, Tanabe Y, Koyama T, Itsui Y, Takeda Y, et al. Suppression of hepatitis C virus replication by cyclosporin a is mediated by blockade of cyclophilins. Gastroenterology 2005;129:1031-1041.
25. Lin Y, Nomura T, Cheong J, Dorjsuren D, Iida K, Murakami S. Hepatitis B virus X protein is a transcriptional modulator that communicates with transcription factor IIB and the RNA polymerase II subunit 5. J Biol Chem 1997;272:7132-7139.
26. Moriya K, Fujie H, Shintani Y, Yotsuyanagi H, Tsutsumi T, Ishibashi K, et al. The core protein of hepatitis C virus induces hepatocellular carcinoma in transgenic mice. Nat Med 1998;4:1065-1067.
27. Lerat H, Honda M, Beard MR, Loesch K, Sun J, Yang Y, et al. Steatosis and liver cancer in transgenic mice expressing the structural and nonstructural proteins of hepatitis C virus. Gastroenterology 2002;122:352-365.
28. Adinolfi LE, Gambardella M, Andreana A, Tripodi MF, Utili R, Ruggiero G. Steatosis accelerates the progression of liver damage of chronic hepatitis C patients and correlates with specific HCV genotype and visceral obesity. HEPATOLOGY 2001;33:1358-1364.
29. Monto A, Alonzo J, Watson JJ, Grunfeld C, Wright TL. Steatosis in chronic hepatitis C: relative contributions of obesity, diabetes mellitus, and alcohol. HEPATOLOGY 2002;36:729-736.
30. Raney AK, Kline EF, Tang H, McLachlan A. Transcription and replication of a natural hepatitis B virus nucleocapsid promoter variant is regulated in vivo by peroxisome proliferators. Virology 2001;289:239-251.
31. Guidotti LG, Eggers CM, Raney AK, Chi SY, Peters JM, Gonzalez FJ, et al. In vivo regulation of hepatitis B virus replication by peroxisome proliferators. J Virol 1999;73:10377-10386.
32. Murakami J, Shimizu Y, Kashii Y, Kato T, Minemura M, Okada K, et al. Functional B-cell response in intrahepatic lymphoid follicles in chronic hepatitis C. HEPATOLOGY 1999;30:143-150.
33. Racanelli V, Sansonno D, Piccoli C, D'Amore FP, Tucci FA, Dammacco F. Molecular characterization of B cell clonal expansions in the liver of chronically hepatitis C virus-infected patients. J Immunol 2001;167:21-29.
34. Guleng B, Tateishi K, Ohta M, Kanai F, Jazag A, Ijichi H, et al. Blockade of the stromal cell-derived factor-1/CXCR4 axis attenuates in vivo tumor growth by inhibiting angiogenesis in a vascular endothelial growth factor-independent manner. Cancer Res 2005;65:5864-5871.

MAJOR ARTICLE

Expression Profiling of Peripheral-Blood Mononuclear Cells from Patients with Chronic Hepatitis C Undergoing Interferon Therapy

Makoto Tateno,[1] Masao Honda,[1] Takashi Kawamura,[2] Hiroyuki Honda,[2] and Shuichi Kaneko[1]

[1]Department of Cancer Gene Regulation, Kanazawa University Graduate School of Medical Science, Kanazawa, and [2]Department of Biotechnology, School of Engineering, Nagoya University, Nagoya, Japan

Background. Interferon (IFN) is now the standard treatment for chronic hepatitis C (CH-C); however, treatment efficacy is unpredictable before IFN therapy is started.

Methods. We investigated the gene-expression profiles of peripheral-blood mononuclear cells (PBMCs) from patients with CH-C showing different responses to IFN. Gene-expression profiles of PBMCs were analyzed in 21 patients with CH-C treated with IFN alone or in combination with ribavirin as well as in 6 healthy volunteers. Serial changes in the gene-expression profiles of PBMCs from individual patients were evaluated before treatment, 2 weeks after the start of IFN therapy, and 6 months after the completion of IFN therapy.

Results. Interestingly, the gene-expression profiles of PBMCs from patients with CH-C and healthy volunteers differed substantially; early T cell–activation antigen CD69 was significantly up-regulated in patients with CH-C, but immune-related molecules such as chemokine (C-C motif) receptor 2 and interleukin 7 receptor were significantly down-regulated. Selected combinations of expressed genes obtained before treatment and during IFN therapy by use of a fuzzy neural network combined with the SWEEP operator method predicted the outcome of IFN therapy with peak accuracies of 91.0% and 90.2%, respectively.

Conclusions. These findings suggest that the gene-expression profiles of PBMCs from patients with CH-C may be useful biomarkers for IFN therapy.

Although interferon (IFN) is currently the standard treatment for patients with chronic hepatitis C (CH-C), only 30%–40% of patients completely eliminate the virus, even after effective IFN and ribavirin combination therapy [1–3]. The mechanism of viral persistence during IFN treatment remains to be clarified. It has been reported that several clinical factors, such as viral load, genotype, degree of fibrosis, and expression of type I IFN receptors, are useful predictive factors for the outcome of IFN therapy [4–6]; however, precise prediction is not possible at present.

Type I IFN, such as IFN-α and IFN-β, plays an important role in innate immunity against viral infections by suppressing viral replication [7, 8]. However, the biological activities of IFN have not been fully elucidated. In viral infections such as measles, the number of peripheral lymphocytes generally decreases. It has also been reported that infection of dendritic cells and other immunocompetent cells is involved in exacerbated disease states and persistent infection [9]. Hence, it may be possible to assess disease state and severity by examining peripheral-blood mononuclear cells (PBMCs) from infected individuals. PBMCs include lymphocytes and monocytes, which play the most important roles in the immunological response to viral infection.

In the present study, we investigated the gene-expression profiles of PBMCs from patients with CH-C and healthy volunteers by use of cDNA microarray techniques [10–16]. By determining the gene-expression profiles of PBMCs from patients with CH-C receiving IFN therapy, we also clarified the differences in the PBMC gene-expression profiles between patients

Received 30 May 2006; accepted 23 August 2006; electronically published XX December 2006.

Potential conflicts of interest: none reported.

Reprints or correspondence: Shuichi Kaneko, Dept. of Cancer Gene Regulation, Kanazawa University Graduate School of Medical Science, 13-1, Takara-Machi, Kanazawa 920-8641, Japan (skaneko@medf.m.kanazawa-u.ac.jp).

The Journal of Infectious Diseases 2007;195:000–000

0022-1899/2007/19502-00XX$15.00

Table 1. Clinical characteristics of patients and responses to interferon (IFN) therapy.

Group, patient (sex, age in years)	ALT level, IU/L	Histology score	Serotype	IFN therapy	Response	Serum HCV RNA level, kIU/mL			PBMC HCV RNA at 2 weeks
						Before	2 weeks	6 months	
Group A									
1 (M, 46)	31	F1/A1	2	Mono	CR	23	<0.5	<0.5	–
2 (F, 47)	40	F1/A1	2	Mono	CR	416	<0.5	<0.5	+
3 (M, 71)	59	F4/A2	1	Mono	CR	42.3	2.2	<0.5	–
4 (M, 55)	19	F4/A2	2	Mono	CR	1.3	<0.5	<0.5	–
5 (M, 54)	30	F2/A1	1	Mono	BR	620	ND	>850	ND
6 (F, 43)	46	F2/A1	1	Mono	BR	160	<0.5	611	+
7 (M, 58)	236	F1-2/A1	NA	Mono	BR	360	<0.5	620	–
8 (M, 60)	114	F3/A2	2	Mono	BR	770	<0.5	2200	–
9 (M, 62)	70	F2/A1	1	Mono	NR	130	130	350	+
10 (M, 42)	59	F2/A1	1	Mono	NR	800	7.2	190	–
11 (F, 62)	138	F2-3/A2	2	Mono	NR	650	183	1400	+
12 (M, 49)	48	F2/A2	2	Mono	NR	330	<0.5	69.5	–
13 (F, 56)	104	F1/A1	1	Mono	NR	751	<0.5	610	–
Group B									
14 (M, 49)	69	F3/A2	1	Combination	CR	>850	ND	<0.5	ND
15 (M, 50)	35	F1/A2	1	Combination	CR	475	<0.5	<0.5	ND
16 (M, 44)	106	F2/A2	1	Combination	NR	325	68.8	82.6	ND
17 (M, 56)	30	F2/A1	1	Combination	CR	91	<0.5	<0.5	ND
18 (F, 39)	47	F1/A1	1	Combination	CR	>850	0.7	<0.5	ND
19 (F, 64)	117	F2/A1	1	Combination	NR	484	0.8	>850	ND
20 (M, 66)	31	F2/A1	1	Combination	NR	>850	390	1300	ND
21 (F, 62)	103	F3/A2	1	Combination	NR	820	270	1200	ND

NOTE. +, positive; –, negative; ALT; alanine aminotransferase; BR, biological responder; CR, complete responder; F, female; M, male; NA; not applicable ND; not detected; NR, nonresponder; PBMC, peripheral-blood mononuclear cell.

with CH-C who responded to IFN therapy (complete responders [CRs]) and those who did not (nonresponders [NRs]).

SUBJECTS, MATERIALS, AND METHODS

Patients. Subjects were 21 patients with CH-C and 7 patients who showed no clinical signs of hepatitis at Kanazawa University Hospital, Japan, between 1999 and 2001. To 13 patients with CH-C (group A), 6 million IUs of IFN-α2b was administered every day for 2 weeks and then 3 times weekly for 22 weeks. To 8 patients with CH-C (group B), IFN-α2b was administered in the same fashion, and ribavirin was administered concomitantly (600 mg for ≤60 kg of body weight, 800 mg for 60–80 kg of body weight, and 1000 mg for >80 kg of body weight). The 6 age- and sex-matched healthy volunteers were seronegative for either hepatitis B surface antigen or hepatitis C virus (HCV) antibody and had liver function values within normal limits. Eight CRs (negative HCV RNA for >6 months), 4 biochemical responders (BRs; normal serum alanine aminotransferase [ALT] levels for >6 months and positive serum HCV RNA), and 9 NRs to IFN therapy were enrolled. After informed consent was obtained from patients, peripheral-blood samples were collected before the start of IFN therapy, at 2 weeks into treatment, and at 6 months after the completion of treatment. PBMCs were then isolated from whole blood and stored in liquid nitrogen until use. Grading and staging of chronic hepatitis were histologically assessed according to the method of Desmet et al. [17]. Clinical characteristics, such as sex, age, ALT levels, degree of histological activity or staging, HCV RNA load and HCV serotype, did not differ significantly among the groups (table 1).

Virological assessment. The amount of HCV RNA was assayed by the Amplicor Monitor Test (Roche Molecular Systems). HCV was classified by a serologic genotyping assay that has been shown to be specific and sensitive for determining HCV genome subtype [18].

Preparation of cDNA microarray slides. Most cDNA clones used in the present study were obtained from IMAGE Consortium libraries through their distributor, Research Genetics, as described elsewhere [19–24]. In addition to these clones, we included clones to monitor IFN signaling. The newly constructed cDNA microarray slide (Kanazawa IFN chip; version 1.0) comprised 400 representative IFN signaling–related genes, 200 receptor- and cell adhesion–related genes, 160 apoptosis- and cell cycle–related genes, 150 transcription factors, 120 stress-response genes, and 275 other functional genes.

RNA isolation and antisense RNA amplification. Total

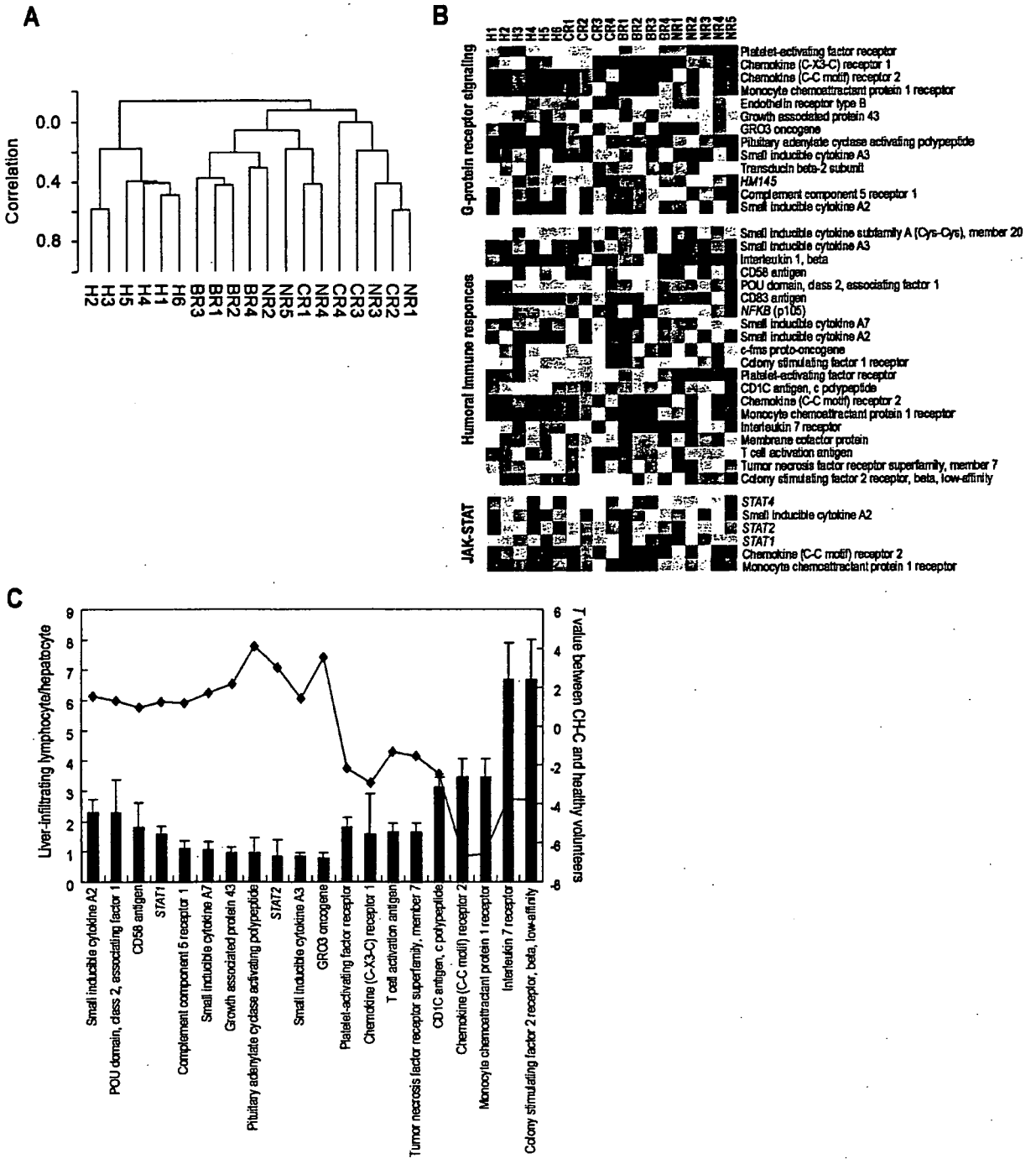

Figure 1. *A,* Hierarchical clustering analysis of gene-expression profiles of peripheral-blood mononuclear cell (PBMC) samples from 13 patients with chronic hepatitis C (CH-C; complete responders [CRs] 1–4, biochemical responders [BRs] 1–4, and nonresponders [NRs] 1–5) and 6 healthy volunteers (H1–H6) among 1305 tested genes before the start of interferon (IFN) therapy, performed using BRB-ArrayTools software. The dendrogram indicates the order in which patients were grouped on the basis of similarities in their gene-expression patterns. *B,* One-way clustering analysis of gene-expression profiles of PBMCs before the start of IFN therapy, using differentially expressed genes in the Janus kinase signal transducer and activation of transcription cascade, humoral immune response, and G protein–coupled receptor protein signaling pathway. Gene cluster data are presented graphically as colored images, red indicates up-regulated genes, and blue indicates down-regulated genes. *C,* Bar graph indicating gene expression in liver-infiltrating lymphocytes relative to that in hepatocytes *(left axis)* and line graph indicating the *T* values for class-prediction analysis between patients with CH-C and healthy volunteers *(right axis).* Genes with increased expression in the liver *(red)* tended to be expressed at lower levels in PBMCs, and genes with decreased expression in the liver *(blue)* tended to be expressed at higher levels in PBMCs.

Table 2. Representative up- or down-regulated genes in patients with chronic hepatitis C, compared with that in healthy volunteers.

Category, gene name	Ratio	*T*	*P*	GenBank accession no.	Gene annotation
Up-regulated					
CD83 antigen (activated B lymphocytes, immunoglobulin superfamily)	3.60	4.26	.00125	NM_004233	Defense response
Thrombospondin 1	3.29	5.19	.00014	NM_003246	Endopeptidase inhibitor activity
CD69 antigen (p60, early T cell–activation antigen)	2.87	5.55	.00001	NM_001781	Transmembrane receptor activity
Regulator of G protein signaling 1	2.33	4.31	.00029	NM_002922	Signal transducer activity
Pituitary adenylate cyclase–activating polypeptide	2.01	4.12	.00046	NM_001117	Neuropeptide hormone activity
Nicotinamide N-methyltransferase	1.99	5.29	.00003	NM_006169	Methyltransferase activity
Clone rasi-1 matrix metalloproteinase RASI-1	1.70	4.56	.00019	NM_002429	Hydrolase activity
VASP exons 4–13	1.68	4.35	.00026	NM_003370	Actin binding
Xeroderma pigmentosum, complementation group A	1.63	3.86	.00085	NM_000380	Damaged DNA binding
Urokinase-type plasminogen activator receptor; GPI-anchored form precursor (*UPAR*); monocyte-activation antigen Mo3; CD87 antigen	1.53	4.41	.00023	NM_002659	Protein binding
Down-regulated					
Chemokine (C-C motif) receptor 2	0.35	−6.69	.00000	NM_000647	C-C chemokine receptor activity
Interleukin 7 receptor	0.47	−3.69	.00129	NM_002185	Antigen binding
Annexin II (lipocortin II)	0.49	−4.86	.00007	NM_004039	Calcium ion binding
Colony stimulating factor 2 receptor β, low-affinity (granulocyte-macrophage)	0.52	−3.85	.00088	NM_000395	Interleukin 3 receptor activity
Cytoplasmic dynein light chain	0.53	−4.12	.00046	NM_003746	Enzyme inhibitor activity
Ribosomal protein L13a	0.55	−3.94	.00070	X56932	Structural constituent of ribosome
Ikaros/LyF-1 homolog	0.56	−4.30	.00029	NM_006060	DNA binding
Chaperonin-containing TCP1, subunit 4 (Δ)	0.56	−4.60	.00014	NM_006430	Unfolded protein binding
Eosinophil Charcot-Leyden crystal (CLC) protein (lysophospholipase)	0.57	−3.73	.00116	NM_001828	Hydrolase activity
Myeloid cell nuclear differentiation antigen	0.57	−3.66	.00138	M81750	DNA binding
Ribosomal protein S16	0.59	−3.84	.00091	M60854	Structural constituent of ribosome
FK506-binding protein 4 (59 kD)	0.62	−4.28	.00030	NM_002014	Isomerase activity
Transforming growth factor β receptor IIB	0.62	−3.87	.00082	NM_003242	Type II transforming growth factor β receptor activity
Ribosomal protein L3	0.62	−3.80	.00099	X73460	Structural constituent of ribosome
KIAA0053	0.63	−5.73	.00001	D29642.1	GTPase activator activity
Peptidylprolyl isomerase D (cyclophilin D)	0.65	−4.71	.00011	NM_005038	FK506 binding
Citrate synthase	0.66	−5.54	.00001	NM_004077	Transferase activity
FADD	0.66	−3.72	.00119	NM_003824	Protein binding
C-myc oncogene	0.66	−3.84	.00089	NM_002467	Transcription factor activity
Interferon regulatory factor 2	0.66	−3.60	.00159	NM_002199	RNA polymerase II transcription factor activity
Intercellular adhesion molecule 3	0.66	−4.30	.00029	NM_002162	Protein binding

Table 3. Gene ontology (GO) comparison to discriminate between patients with chronic hepatitis C and healthy volunteers.

GO category	GO description	Genes, no.	*P* LS permutation	*P* KS permutation
7259	JAK-STAT cascade	6	.00167	.17913
6959	Humoral immune response	25	.00303	.03114
7186	G protein–coupled receptor protein signaling pathway	18	.00348	.17617

NOTE. JAK-STAT, Janus kinase signal transducer and activation of transcription.

RNA from PBMCs was isolated using Micro RNA Isolation Kits (Stratagene), and antisense RNA (aRNA) was amplified as described elsewhere [20, 22, 24]. The quality and degradation of isolated RNA were estimated after electrophoresis using an Agilent 2001 bioanalyzer. The references used for each microarray analysis were aRNA samples prepared from PBMCs obtained from a volunteer. Microarray hybridization was performed as described elsewhere [19–24], and each hybridization was repeated for all samples.

Gene-expression profiles of liver-infiltrating lymphocytes in patients with CH-C were investigated by laser-capture microdissection (LCM). Infiltrated lymphoid cells in the portal area and hepatocytes in liver-biopsy specimens obtained from 8 patients with CH-C were isolated by LCM. After 2 rounds of total

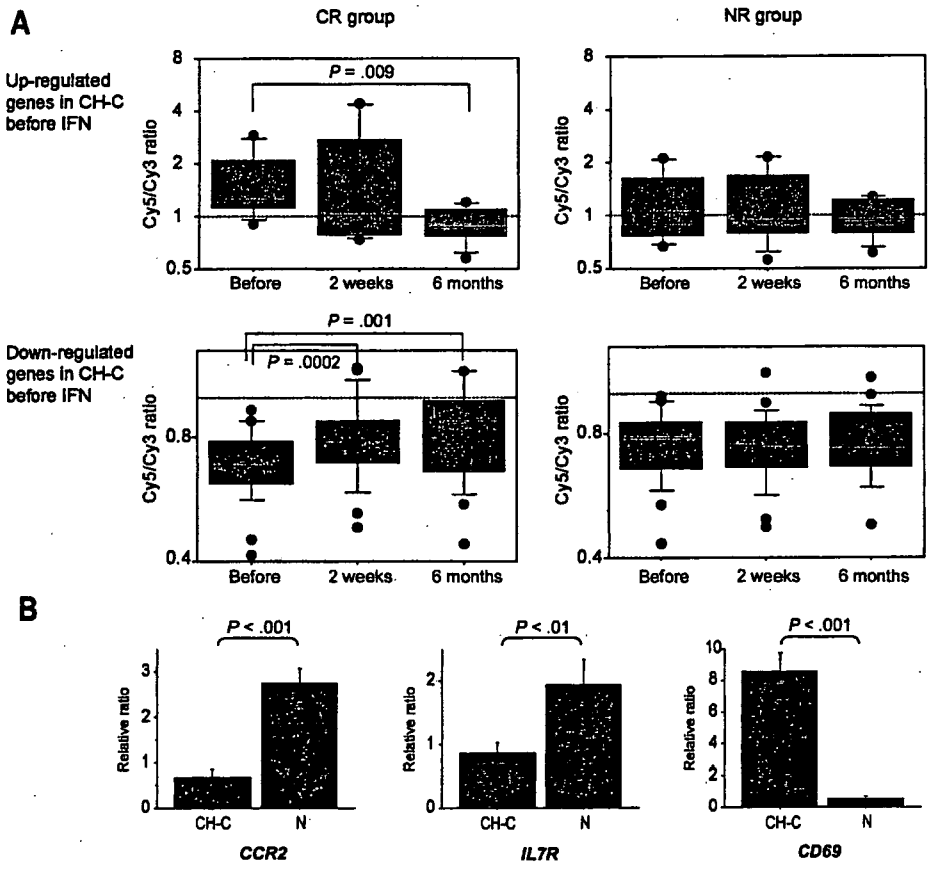

Figure 2. *A*, Changes in gene-expression profiles over the course of interferon (IFN) therapy (as shown in table 2) distinguishing patients with chronic hepatitis C (CH-C) from healthy volunteers before the start of IFN therapy. Box charts show average rates of change in relation to healthy volunteers as index functions. *B*, Real-Time polymerase chain reaction data for *CCR2* and *IL7R*, which were down-regulated (as determined on the basis of microarray data) in patients with CH-C before the start of IFN therapy, and *CD69*, which was up-regulated in patients with CH-C.

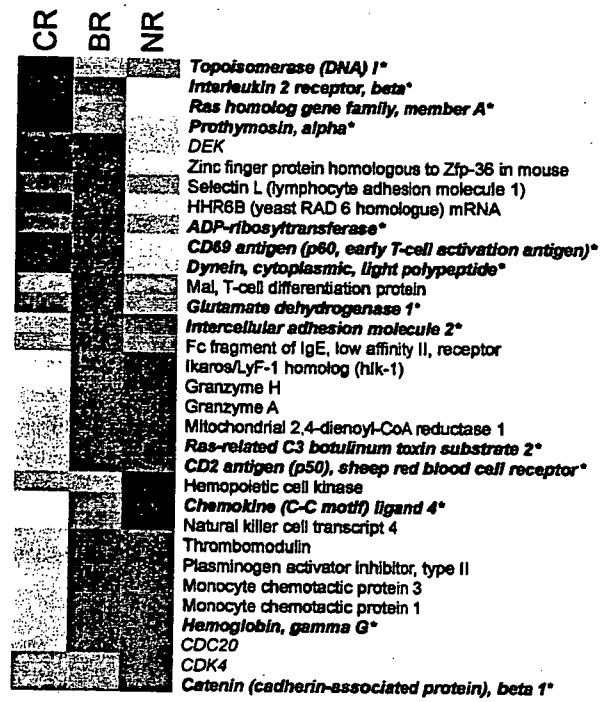

Figure 3. Thirty-two genes screened for gene-expression data before interferon (IFN) therapy by projective adaptive resonance theory. Red indicates up-regulated genes, and blue indicates down-regulated genes. Asterisks indicate genes that present similar expression patterns during IFN and ribavirin combination therapy. BR, biochemical responder; CR, complete responder; NR, nonresponder.

RNA amplification, the gene expression in infiltrated lymphoid cells was compared with that in hepatocytes [25]. Optimal conditions for LCM and reproducibility of data were assessed repeatedly [24, 25]. Some of these data were used for the analysis of genes expression.

Image analysis and data processing. Quantitative assessment of signals on the slides was performed using a ScanArray 5000 device (General Scanning), followed by image analysis q11 using QuantArray software (General Scanning).

Hierarchical clustering of gene expression in patients was performed using BRB-ArrayTools software (available at: http:/ q12 /linus.nci.nih.gov/BRB-ArrayTools.html). Filtered data were log transferred, normalized, centered, and applied to the average linkage clustering with centered correlation. BRB-ArrayTools include class comparison and class prediction tools based on univariate *F* tests to identify genes differentially expressed between predefined clinical groups. The permutation distribution of the *F* statistic, based on 2000 random permutations, was also used to confirm statistical significance. $P < .05$, as well as >1.5-fold differences in gene expression, were considered to be significant. A gene ontology (GO) comparison tool provides a list that has more genes differentially expressed and is coordinately regulated among predefined clinical groups than expected by chance and enables findings among biologically related genes to reinforce one another. Fisher and Kolmogorov-Smirnov tests were performed for GO comparison ($P < .005$) (BRB-ArrayTools).

Changes in gene expression in patients receiving IFN therapy were classified on the basis of self-organizing maps (GeneCluster software; version 2.0; available at: http://www.broad.mit.edu/cancer/software/genecluster2/gc2.html).

To identify class predictor genes for IFN therapy, projective adaptive resonance theory (PART) was used as a screening method for cDNA microarray data; unlike conventional clustering methods, PART enables the elimination of nonspecific dimensions for clustering from high-dimensional data [28–30]. From the genes extracted by PART, class predictor genes were selected using a fuzzy neural network (FNN) combined with the SWEEP operator method (FNN-SWEEP method). An FNN model with 1 input unit was initially created. Expression data for genes from data sets for patients with CH-C were entered into the FNN model, and the weight parameter was determined by the SWEEP operator method. We repeated this procedure for all genes to construct a model for each gene. The 10 genes with the highest accuracy levels were selected as the "first gene." The parameter increasing method was then applied. Having the first gene fixed, we used a similar method to select the second gene, which gave the highest accuracy in combination with the

Table 4. Ten gene combinations selected by the SWEEP operator method for construction of chronic hepatitis C class prediction at the start of interferon (IFN) therapy.

Combination	Input	Gene name	GenBank accession no.	Accuracy, %	
				Training	Test
1	1	***CD2 antigen (p50), sheep red blood cell receptor*** [a]	NM_001767	21.2	14.1
	2	Glutamate dehydrogenase 1	NM_005271	72.4	46.2
	3	Dynein, cytoplasmic, light polypeptide	NM_003746	55.8	49.4
2	1	Ras-related C3 botulinum toxin substrate 2	NM_002872	34.6	20.5
	2	Glutamate dehydrogenase 1	NM_005271	81.4	68.6
	3	***Interleukin 2 receptor β*** [a]	NM_000878	53.2	43.6
3	1	***Hemoglobin γG*** [a]	NM_000184	19.9	16.7
	2	Ras-related C3 botulinum toxin substrate 2	NM_002872	64.7	36.6
	3	Dynein, cytoplasmic, light polypeptide	NM_003746	62.2	58.3
4	1	Intercellular adhesion molecule 2	NM_000873	28.9	26.3
	2	Ras homolog gene family member A	NM_001664	41.7	25.7
	3	Prothymosin α	NM_002823	66.0	47.4
5	1	Topoisomerase (DNA) I	NM_003286	53.9	46.2
	2	Catenin (cadherin-associated protein) β1 (88 kD)	NM_001904	66.0	57.1
	3	Ras-related C3 botulinum toxin substrate 2	NM_002872	91.0	89.1
6	1	Catenin (cadherin-associated protein) β1 (88 kD)	NM_001904	44.9	41.0
	2	Topoisomerase (DNA) I	NM_003286	66.0	57.1
	3	Ras-related C3 botulinum toxin substrate 2	NM_002872	91.0	89.1
7	1	Catenin (cadherin-associated protein) β1 (88 kD)	NM_001904	35.3	31.4
	2	***Interleukin 2 receptor β*** [a]	NM_000878	47.4	43.6
	3	ADP-ribosyltransferase (NAD+; poly [ADP-ribose] polymerase)	NM_001618	62.2	60.9
8	1	Chemokine (C-C motif) ligand 4	NM_002984	44.9	41.0
	2	***Interleukin 2 receptor β*** [a]	NM_000878	37.8	29.5
	3	Topoisomerase (DNA) I	NM_003286	44.9	34.6
9	1	***Interleukin 2 receptor β*** [a]	NM_000878	30.8	30.8
	2	Catenin (cadherin-associated protein) β1 (88 kD)	NM_001904	47.4	43.6
	3	ADP-ribosyltransferase (NAD+; poly [ADP-ribose] polymerase)	NM_001618	62.2	60.9
10	1	CD69 antigen (p60, early T cell–activation antigen)	NM_001781	42.3	32.1
	2	Prothymosin α	NM_002823	33.3	24.4
	3	Glutamate dehydrogenase 1	NM_005271	39.1	31.4

[a] Genes that present similar expression patterns during IFN and ribavirin combination therapy.

first gene. Having the first gene and the second gene fixed, we selected the third gene. For validation of this model, we performed leave-one-out cross-validation (LOOCV); we left out 1 test sample and used the remaining 12 samples as training samples. We created 13 such sets. The FNN model was built up for 12 test samples, and the accuracy of training and test samples was calculated.

Real-time quantitative reverse-transcription polymerase chain reaction (RT-PCR). Quantitation of chemokine (C-C motif) receptor 2 *(CCR2)*, *CD69*, and interleukin 7 receptor *(IL7R)* RNA expression was performed using the TaqMan real-rime PCR assay (ABI PRISM 7700 Sequence Detection System; PE Applied Biosystems), as described elsewhere [22, 23].

Statistical analysis. All data are expressed as mean ± SE values. One-way analysis of variance by the Bonferroni method or Student's *t* test was used to determine the significance of differences in clinical characteristics between patients in this study. $P < .05$ was considered to be significant.

RESULTS

cDNA microarray analysis of expression profiles of PBMCs from patients with CH-C. We initially compared the PBMC gene-expression profiles of patients with CH-C with those of healthy volunteers. For all 1305 genes, the results of hierarchical clustering analysis, a nonsupervised learning method, confirmed that the gene-expression profiles of PBMCs from the 6 healthy volunteers clearly differed when compared with those of the 13 patients with CH-C (group A) before IFN therapy (figure 1*A*). When the 2 groups were compared by support

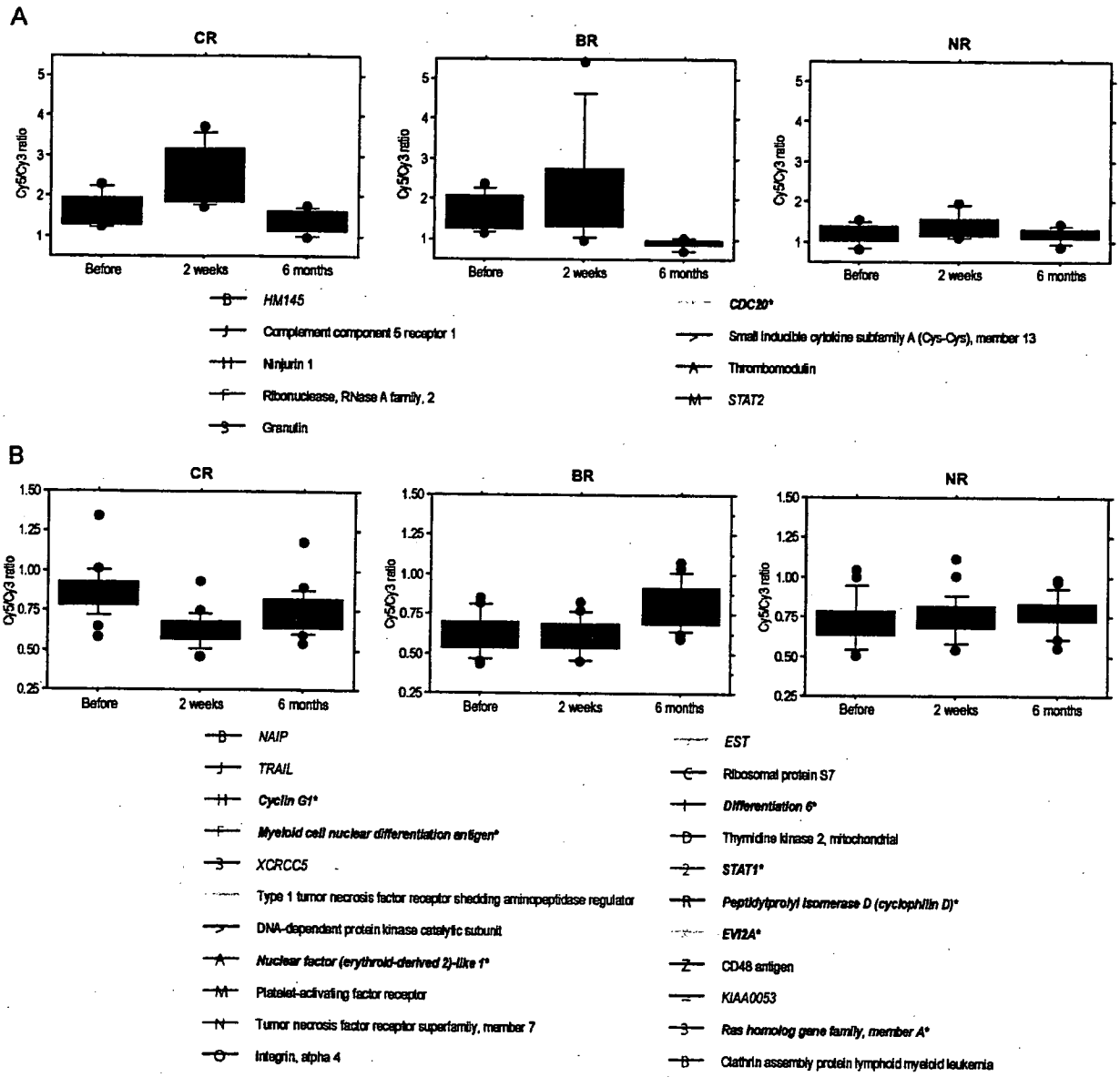

Figure 4. Gene-expression patterns. By use of projective adaptive resonance theory, 86 genes with changes in gene expression before and 2 weeks after the start of interferon (IFN) therapy were selected. For the complete responder (CR) group, changes in the expression of the 86 genes due to IFN therapy were classified into the following 5 patterns, on the basis of self-organizing maps (GeneCluster): up-regulated at 2 weeks after the start of IFN therapy and then down-regulated after the end of IFN therapy *(A)*; down-regulated at 2 weeks after the start of IFN therapy and then up-regulated after the end of IFN therapy *(B)*; up-regulated at 2 weeks after the start of IFN therapy and also up-regulated after the end of IFN therapy *(C)*; up-regulated at 2 weeks after the start of IFN therapy and then returned to normal after the end of IFN therapy *(D)*; and down-regulated at 2 weeks after the start of IFN therapy and also down-regulated after the end of IFN therapy *(E)*. Representative genes are listed under each pattern. Asterisks indicate genes that present similar expression patterns during IFN and ribavirin combination therapy.

vector machine, a supervised learning method (BRB-ArrayTools), a total of 48 predictor genes were identified with a significance level of $P < .002$, and it was possible to differentiate the 2 groups with 100% accuracy. Gene parameters (ratio, T value, P value, description, GenBank accession no., and annotation) are summarized in table 2. q13

A GO comparison tool (BRB-ArrayTools) identifies more genes that are differentially expressed and are coordinately reg-

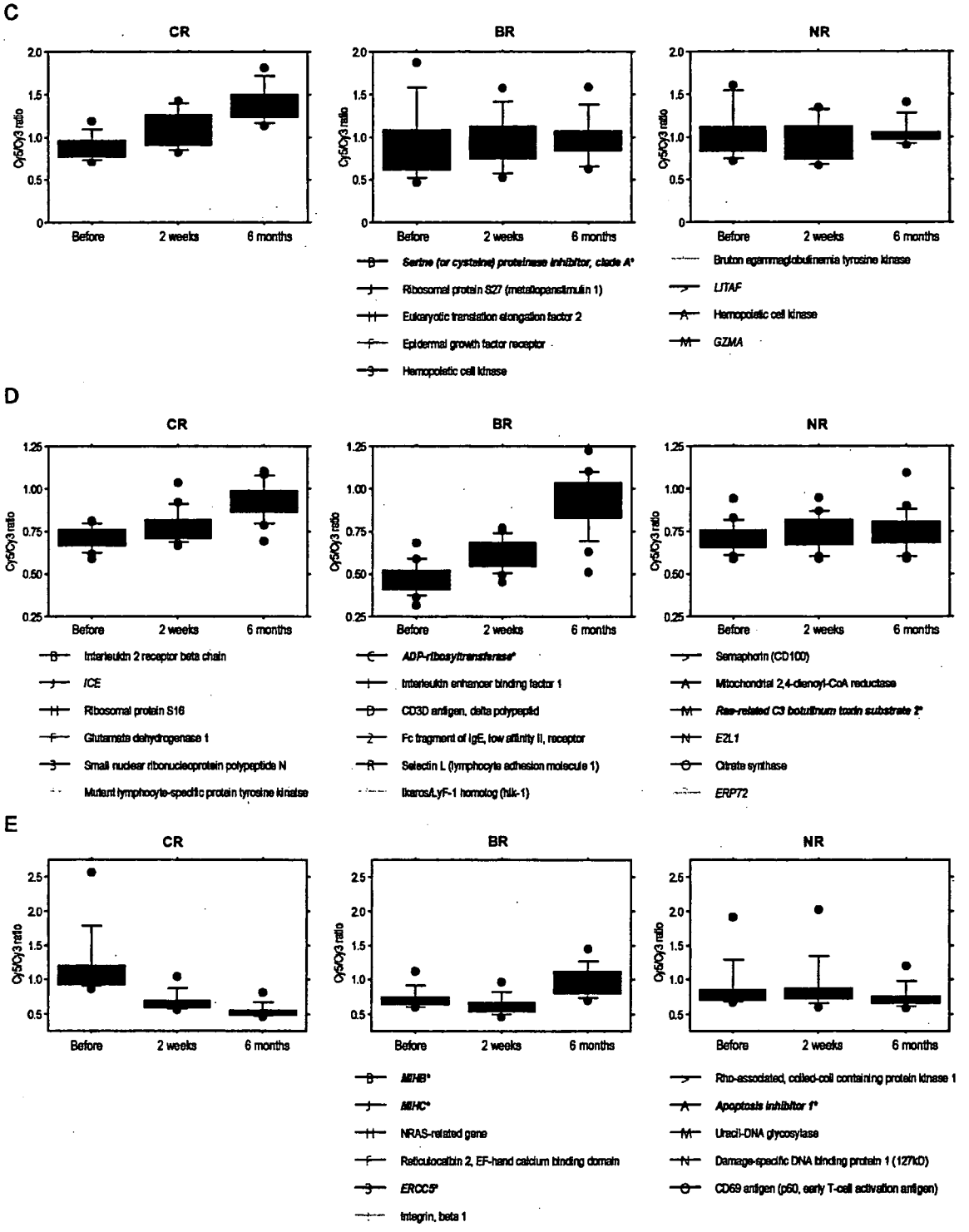

Figure 4. *(Continued.)*

Table 5. Ten gene combinations selected by the SWEEP operator method for the construction of chronic hepatitis C class prediction 2 weeks after the start of interferon (IFN) therapy.

Combination	Input	Gene name	GenBank accession no.	Accuracy, %	
				Training	Test
1	1	*ERCC5*	NM_000123	55.3	45.5
	2	Serine (or cysteine) proteinase inhibitor clade A member 1	NM_000295	85.6	54.5
	3	Ras homolog gene family member A	NM_001664	80.3	70.5
2	1	Baculoviral IAP repeat–containing 2	NM_001166	47.7	41.7
	2	Serine (or cysteine) proteinase inhibitor clade A member 1	NM_000295	80.3	53.8
	3	Ras homolog gene family member A	NM_001664	80.3	70.5
3	1	Cyclin G1	NM_004060	36.6	44.0
	2	Ras-related C3 botulinum toxin substrate 2	NM_002872	79.6	61.4
	3	*EST*		70.5	56.8
4	1	Ecotropic viral integration site 2A	NM_001003927	41.7	25.8
	2	Peptidylprolyl isomerase D (cyclophilin D)	NM_005038	60.6	46.2
	3	Cyclin G1	NM_004060	77.3	67.4
5	1	***Myeloid cell nuclear differentiation antigen***[a]	NM_002432	55.3	25.8
	2	Cyclin G1	NM_004060	85.6	64.4
	3	ADP-ribosyltransferase (NAD+; poly [ADP-ribose] polymerase)	NM_001618	80.3	87.1
6	1	Integrin β1	NM_033666	47.7	19.7
	2	Cyclin G1	NM_004060	80.3	62.9
	3	***STAT1AB***[a]	NM_139266	80.3	68.2
7	1	Differentiation 6 (septin 2)	NM_004404	28.8	25.8
	2	Cyclin G1	NM_004060	75.0	64.4
	3	Cell division cycle 20 homolog *(S. cerevisiae)*	NM_001255	90.2	87.9
8	1	*MIHC*	NM_001165	28.8	25.0
	2	Cyclin G1	NM_004060	75.0	64.4
	3	Cell division cycle 20 homolog *(S. cerevisiae)*	NM_001255	90.2	87.9
9	1	Apoptosis inhibitor 1 (baculoviral IAP repeat–containing 3)	NM_001165	28.8	25.0
	2	Cyclin G1	NM_004060	75.0	64.4
	3	Cell division cycle 20 homolog *(S. cerevisiae)*	NM_001255	90.2	87.9
10	1	Nuclear factor (erythroid-derived 2)–like 1	NM_003204	25.0	25.8
	2	Cyclin G1	NM_004060	75.0	63.6
	3	ADP-ribosyltransferase (NAD+; poly [ADP-ribose] polymerase)	NM_001618	88.6	81.8

[a] Genes that present similar expression patterns during IFN and ribavirin combination therapy

ulated among predefined clinical groups than expected by chance, thus enabling the finding of biologically related genes to reinforce one another. GO comparison of gene expression between the patients with CH-C and the healthy volunteers revealed significant differences in the Janus kinase signal transducer and activation of transcription (JAK-STAT) cascade, humoral immune response, and G protein–coupled receptor protein signaling pathway ($P < .005$) (table 3). One-way clustering analyses of representative differentially expressed genes are shown in figure 1*B*. These genes were generally activated in PBMCs from patients with CH-C; however, genes such as *CCR2*, monocyte chemoattractant protein 1 receptor, and *IL7R* were significantly down-regulated. The reason for this is not known, but it may reflect infiltration of PMBCs into the liver. The top 20 differentially expressed genes were selected, and gene-expression profiling of these genes in liver-infiltrating lymphocytes was performed (figure 1*C*). Most of the gene-expression ratios for liver-infiltrating lymphocytes showed >1-fold increases compared with hepatocytes, thus indicating that most genes were preferentially expressed in lymphocytes. Interestingly, the genes with increased expression in liver-infiltrating lymphocytes tended to be expressed at lower levels in PBMCs (figure 1*C*).

Serial changes in the differentially expressed genes listed in table 2 during IFN treatment are shown in figure 2*A*. In the CR group, the expression profiles of genes that were either up-

Table 6. Comparison of ISG expression induced by interferon (IFN).

The table is available in its entirety in the online edition of the *Journal of Infectious Diseases*.

or down-regulated before IFN therapy were similar to those of healthy volunteers 6 months after the end of IFN therapy (figure 2*A*, CR group). On the other hand, in the NR group, expression of genes that were either up- or down-regulated before IFN therapy tended to remain up- or down-regulated 6 months after the end of IFN therapy (figure 2*A*, NR group). This suggests that the changes in gene-expression profiles of patients with CH-C before IFN therapy reflect the state of HCV infection.

We performed real-time PCR to corroborate the microarray data. Real-time PCR revealed that *CD69* was up-regulated in patients with CH-C and that *CCR2* and *IL7R* were down-regulated in patients with CH-C (figure 2*B* and table 2).

Relationship between PBMC gene-expression profiles and IFN response. We then analyzed the relationship between PBMC gene-expression profiles before the start of IFN therapy and IFN response. Because the regimen of IFN treatment was different in group A and group B patients, we first focused on group A patients (table 1). In hierarchical clustering analysis using all genes before IFN therapy, no clustering was seen in the CR, BR, or NR groups. Conventional supervised learning methods, such as support vector machine and nearest neighbor (BRB-ArrayTools), could not discriminate between the CR, BR, and NR groups. Therefore, we applied the FNN-SWEEP method to predict the outcome of IFN therapy. Before FNN-SWEEP analysis, nonspecific genes or genes with errors were eliminated by the PART method. The 32 genes screened by q15 PART are shown in figure 3. Topoisomerase (DNA) I *(TOP1)* and interleukin 2 receptor β *(IL2RB)* were up-regulated in the CR group, hemoglobin γG *(HBG2)* and monocyte chemotactic protein were up-regulated in the BR group, and chemokine (C-C motif) ligand 4 and ras-related C3 botulinum toxin substrate 2 *(RAC2)* were up-regulated in the NR group. Genes selected by PART were subjected to the FNN-SWEEP method to construct a class prediction model. Consequently, we selected 10 gene combinations by the SWEEP operator method for CH-C class prediction before the start of IFN therapy (table 4). The most effective gene combination for the prediction of an IFN q16 response was *TOP1;* catenin (cadherin-associated protein) β1 (88 kD); and *RAC2.* The accuracy of the training and test sets were high, at 91.0% and 89.1%, respectively.

Changes in gene-expression profiles over the course of IFN therapy. We next focused on the changes in gene-expression profiles over the course of IFN therapy and their relationship with IFN response. Using PART, 86 genes with changes in expression between before and 2 weeks after the start of IFN therapy were selected. To investigate the relationship between the 86 genes with changes due to IFN therapy and the efficacy of IFN therapy, changes in the expression of the 86 genes were determined for the CR group. On the basis of self-organizing maps, changes in gene expression in the CR group were classified into the following 5 patterns (figure 4): pattern A, up- q17 regulated 2 weeks after the start of IFN therapy and then down-regulated after the end of IFN therapy; pattern B, down-regulated 2 weeks after the start of IFN therapy and then up-regulated after the end of IFN therapy; pattern C, up-regulated 2 weeks after the start of IFN therapy and also up-regulated after the end of IFN therapy; pattern D, up-regulated at 2 weeks after the start of IFN therapy and then returned to normal after the end of IFN therapy; and pattern E, down-regulated at 2 weeks after the start of IFN therapy and also down-regulated after the end of IFN therapy. Patterns A and B represent gene groups with temporary changes during IFN therapy, whereas patterns C, D, and E represent gene groups with changes after the end of IFN therapy and are thought to be attributable to viral eradication or normalization of hepatic function. Interestingly, very little change was seen in the patterns for the NR group. Therefore, changes in gene expression are also useful in predicting therapeutic efficacy. From the 86 genes isolated by PART, the SWEEP operator method was used to identify 10 gene combinations, and therapeutic efficacy was predicted according to the FNN-SWEEP method (table 5). The results showed that the accuracy for gene combinations 7, 8, and 9 was high, at 90.2%. LOOCV confirmed the high accuracy (87.9%) of prediction using these gene combinations. These combinations included the following genes that are important for predicting therapeutic efficacy: *CDC20* was classified as belonging to pattern A; cyclin G1 and differentiation 6 were as belonging to pattern B; and *MIHC* and apoptosis inhibitor 1 were as belonging to pattern E (figure 4).

IFN and ribavirin combination therapy. We then investigated the usefulness of the above-mentioned genes in predicting the efficacy of IFN and ribavirin combination therapy. It has been shown that concurrent ribavirin administration improves the rate of CR. In addition, the changes in gene expression during combination therapy are due not only to IFN but also to ribavirin. Thus, the results for monotherapy may not be applicable to combination therapy. However, changes in the expression of several genes—CD2 antigen (p50), q18 *IL2RB, HBG2,* myeloid cell nuclear differentiation antigen *(MNDA),* and *STAT1AB*—were shown to be extremely useful for distinguishing CR from NR in IFN and ribavirin combination therapy (tables 3 and 4). q19

DISCUSSION

HCV load, genotype, and fibrosis have been listed as factors that influence the effectiveness of IFN therapy [4, 5], but these factors are not sufficient, and other predictive factors are needed. Unlike liver-biopsy specimens, PBMCs can be easily collected, and collection can be repeated as necessary. We analyzed the gene-expression profiles of PBMCs in patients with CH-C by use of cDNA microarrays under the hypothesis that

gene expression in PBMCs is indicative of IFN efficacy and CH-C disease state. In addition, changes in the gene-expression profiles of PBMCs were analyzed during the course of IFN therapy to clarify the relationship between gene-expression profiles of PBMCs and IFN response.

Interestingly, the gene-expression profiles of PBMCs from patients with CH-C and from healthy volunteers were different, and this was confirmed by hierarchical clustering analysis and supervised learning analysis using support vector machine. When patients with CH-C and healthy volunteers were compared, gene expression in the JAK-STAT cascade, humoral immune response, and G protein–coupled receptor protein signaling pathway differed markedly. In most patients with CH-C, expression of these genes is activated, and HCV infection is thought to bring about changes in the gene expression in PBMCs. Several chemokine- and cytokine-related genes, such as *CCR2* and *IL7R*, were down-regulated. Although the reason for this was not clear, expression of these genes in liver-infiltrating lymphocytes was up-regulated. Therefore, the down-
q20 regulation of immune-related genes may represent increased levels of liver-infiltrating lymphocytes accompanying hepatitis. Interestingly, when the chronological changes in PBMC gene-expression profiles were analyzed for the CR group, the profiles at 6 months after the end of therapy were similar to those of healthy volunteers. Therefore, the changes in gene-expression profiles before IFN therapy were due to HCV infection. On the other hand, the gene-expression profiles of the NR group before IFN therapy were similar to those at 6 months after the end of IFN therapy (figure 2*A*).

Unfortunately, it was not possible to differentiate between CR, BR, and NR patients on the basis of gene-expression profiles of PBMCs by use of nonsupervised learning methods, such as hierarchical clustering, before IFN therapy. Therefore, we used FNN theory for CH-C class prediction. The most attractive feature of FNN is that causality between input and output variables can be described very accurately as explicit if-then roles obtained from the constructed model. For the purpose of analyzing numerous genes in a short time, FNN combined with the SWEEP operator method was developed (FNN-SWEEP method) and has been shown to be a precise, simple tool for predicting patient survival on the basis of microarray data [28, 29]. In addition, by first filtering genes by use of PART, the accuracy of the FNN-SWEEP method was further increased [30]. In the present study, a total of 32 genes were identified by PART on the basis of genetic changes before therapy, and, in the CR group, expression of genes such as *TOP1*,
q21 *IL2RB*, prothymosin α (*PTMA*), and ADP-ribosyltransferase was up-regulated, thus indicating active cellular proliferation. In the NR group, the expression of genes indicating activated cytotoxic T cells—such as granzyme, CD2 antigen, *RAC2*, and natural killer cell transcript 4—was up-regulated. Because these genes were up-regulated by IFN therapy in the CR group, they were thought to be up-regulated before therapy in the NR group. Lempicki et al. reported elevated expression of endog- q22
enous IFN/innate immune response genes in PBMCs from NR patients coinfected with HCV and HIV [31]. This suggests that, in many NR patients, few immune effector cells are active or that these effector cells cannot infiltrate the liver and remain in the peripheral blood.

To further investigate the above-mentioned points, changes in the gene-expression profiles of PBMCs were determined during the course of IFN therapy. On the basis of expression profiles before and 2 weeks after the start of IFN therapy, 86 genes were selected. These genes did not include as many IFN-α–stimulated genes as were noted in liver [25–27] (table 6), but q23
they included valuable immune regulatory genes.

On the basis of self-organizing maps, changes in gene expression in the CR group were then classified into 5 patterns (figure 4). These gene groups represent genes with temporary changes due to IFN therapy and those with changes after the end of IFN therapy. Gene groups with changes after the end of IFN therapy are thought to be involved in viral eradication or the normalization of hepatic function. Interestingly, little change was seen in any of the patterns in the NR group. In efficacy prediction by the FNN-SWEEP method, the accuracy for the gene combinations 7, 8, and 9 was high, at 90.2%, thus suggesting that changes in gene expression 2 weeks after the start of IFN therapy are also useful in predicting therapeutic efficacy.

We also investigated whether these genes are useful in predicting the efficacy of IFN and ribavirin combination therapy. Changes in gene expression during combination therapy were due not only to IFN but also to ribavirin, and the results for monotherapy could not simply be applied to combination therapy. However, changes in the expression of several genes—CD2 antigen (p50), *IL2RB*, *HBG2*, *MNDA*, and *STAT1AB*—were shown to be extremely useful for distinguishing CR from NR in IFN and ribavirin combination therapy.

Unfortunately, because the number of subjects in the present study was small, the genes that were identified as predictors for IFN monotherapy were not necessarily predictors for IFN and ribavirin combination therapy. However, the present study was the first to show that responses to IFN therapy could be predicted on the basis of changes in gene expression by PBMCs, and further investigations in greater numbers of patients are required.

Acknowledgments

We thank Prof. Kenichi Kobayashi, for helpful discussion and advice. We also thank A. Nakano, M. Ueda, and J. Hara, for their valuable technical assistance.

References

1. McHutchison JG, Gordon SC, Schiff ER, et al. Interferon alfa-2b alone or in combination with ribavirin as initial treatment for chronic hepatitis C. Hepatitis Interventional Therapy Group. N Engl J Med 1998;339:1485–92.
2. Davis GL, Esteban-Mur R, Rustgi V, et al. Interferon alfa-2b alone or in combination with ribavirin for the treatment of relapse of chronic hepatitis C. International Hepatitis Interventional Therapy Group. N Engl J Med 1998;339:1493–99.
3. Poynard T, Marcellin P, Lee SS, et al. Randomised trial of interferon alpha2b plus ribavirin for 48 weeks or for 24 weeks versus interferon alpha2b plus placebo for 48 weeks for treatment of chronic infection with hepatitis C virus. International Hepatitis Interventional Therapy Group. Lancet 1998;352:1426–32.
4. Martinot-Peignoux M, Marcellin P, Pouteau M, et al. Pretreatment serum hepatitis C virus RNA levels and hepatitis C virus genotype are the main and independent prognostic factors of sustained response to interferon alfa therapy in chronic hepatitis C. Hepatology 1995;22:1050–6.
5. Tsubota A, Chayama K, Ikeda K, et al. Factors predictive of response to interferon-alpha therapy in hepatitis C virus infection. Hepatology 1994;19:1088–94.
6. Mizukoshi E, Kaneko S, Yanagi M, et al. Expression of interferon alpha/beta receptor in the liver of chronic hepatitis C patients. J Med Virol 1998;56:217–23.
7. Ortaldo JR, Mantovani A, Hobbs D, Rubinstein M, Pestka S, Herberman RB. Effects of several species of human leukocyte interferon on cytotoxic activity of NK cells and monocytes. Int J Cancer 1983;31:285–9.
8. Tsubouchi E, Akbar SM, Horiike N, Onji M. Infection and dysfunction of circulating blood dendritic cells and their subsets in chronic hepatitis C virus infection. J Gastroenterol 2004;39:754–62.
9. Popov S, Chenine AL, Gruber A, Li PL, Ruprecht RM. Long-term productive human immunodeficiency virus infection of CD1a-sorted myeloid dendritic cells. J Virol 2005;79:602–8.
10. Schena M, Shalon D, Davis RW, Brown PO. Quantitative monitoring of gene expression patterns with a complementary DNA microarray. Science 1995;270:467–70.
11. Schena M, Shalon D, Heller R, Chai A, Brown PO, Davis RW. Parallel human genome analysis: microarray-based expression monitoring of 1000 genes. Proc Natl Acad Sci USA 1996;93:10614–9.
12. DeRisi J, Penland L, Brown PO, et al. Use of a cDNA microarray to analyse gene expression patterns in human cancer. Nat Genet 1996;14:457–60.
13. Khan J, Simon R, Bittner M, et al. Gene expression profiling of alveolar rhabdomyosarcoma with cDNA microarrays. Cancer Res 1998;58:5009–13.
14. Iyer VR, Eisen MB, Ross DT, et al. The transcriptional program in the response of human fibroblasts to serum. Science 1999;283:83–7.
15. Heller RA, Schena M, Chai A, et al. Discovery and analysis of inflammatory disease-related genes using cDNA microarrays. Proc Natl Acad Sci USA 1997;94:2150–5.
16. Alizadeh AA, Eisen MB, Davis RE, et al. Distinct types of diffuse large B-cell lymphoma identified by gene expression profiling. Nature 2000;403:503–11.
17. Desmet VJ, Gerber M, Hoofnagle JH, Manns M, Scheuer PJ. Classification of chronic hepatitis: diagnosis, grading and staging. Hepatology 1994;19:1513–20.
18. Tanaka T, Tsukiyama-Kohara K, Yamaguchi K, et al. Significance of specific antibody assay for genotyping of hepatitis C virus. Hepatology 1994;19:1347–53.
19. Kawai HF, Kaneko S, Honda M, Shirota Y, Kobayashi K. Alpha-fetoprotein-producing hepatoma cell lines share common expression profiles of genes in various categories demonstrated by cDNA microarray analysis. Hepatology 2001;33:676–91.
20. Honda M, Kaneko S, Kawai H, Shirota Y, Kobayashi K. Differential gene expression between chronic hepatitis B and C hepatic lesion. Gastroenterology 2001;120:955–66.
21. Shirota Y, Kaneko S, Honda M, Kawai HF, Kobayashi K. Identification of differentially expressed genes in hepatocellular carcinoma with cDNA microarrays. Hepatology 2001;33:832–40.
22. Honda M, Shimazaki T, Kaneko S. La protein is a potent regulator of replication of hepatitis C virus in patients with chronic hepatitis C through internal ribosomal entry site-directed translation. Gastroenterology 2005;128:449–62.
23. Kawaguchi K, Honda M, Yamashita T, Shirota Y, Kaneko S. Differential gene alteration among hepatoma cell lines demonstrated by cDNA microarray-based comparative genomic hybridization. Biochem Biophys Res Commun 2005;329:370–80.
24. Honda M, Kawai H, Shirota Y, Yamashita T, Kaneko S. Differential gene expression profiles in stage I primary biliary cirrhosis. Am J Gastroenterol 2005;100:2019–30.
25. Honda M, Yamashita T, Ueda T, Takatori H, Nishino R, Kaneko S. Different signaling pathways in the livers of patients with chronic hepatitis B or chronic hepatitis C. Hepatology 2006;44:1122–38. q24
26. Smith MW, Walters KA, Korth MJ, et al. Gene expression patterns that correlate with hepatitis C and early progression to fibrosis in liver transplant recipients. Gastroenterology 2006;130:179–87.
27. Bigger CB, Guerra B, Brasky KM, et al. Intrahepatic gene expression during chronic hepatitis C virus infection in chimpanzees. J Virol 2004;78:13779–92.
28. Ando T, Suguro M, Kobayashi T, Seto M, Honda H. Selection of casual gene sets for lymphoma prognostication from expression profiling and construction of prognostic fuzzy neural network models. J Biosci Bioeng 2003;96:161–7.
29. Ando T, Suguro M, Kobayashi T, Seto M, Honda H. Multiple fuzzy neural network system for outcome prediction and classification of 220 lymphoma patients on the basis of molecular profiling. Cancer Sci 2003;94:906–13.
30. Takahashi H, Kobayashi T, Honda H. Construction of robust prognostic predictors by using projective adaptive resonance theory as a gene filtering method. Bioinformatics 2005;21:179–86.
31. Lempicki RA, Polis MA, Yang J, et al. Gene expression profiles in hepatitis C virus (HCV) and HIV coinfection: class prediction analyses before treatment predict the outcome of anti-HCV therapy among HIV-coinfected persons. J Infect Dis 2006;193:1172–7.

Liver International 2006: 26: 291–297

Liver International
DOI: 10.1111/j.1478-3231.2005.01231.x

Clinical Studies

The development and clinical features of splenic aneurysm associated with liver cirrhosis

Sunagozaka H, Tsuji H, Mizukoshi E, Arai K, Kagaya T, Yamashita T, Sakai A, Nakamoto Y, Honda M, Kaneko S. The development and clinical features of splenic aneurysm associated with liver cirrhosis.
Liver International 2006: 26: 291–297.

Abstract: *Objectives:* Splenic artery aneurysm (SAA) is usually asymptomatic, but can be fatal if it ruptures. Portal hypertensive patients with varix or splenomegaly are sometimes complicated by SAA. However, there have been no large-scale clinical studies regarding whether liver cirrhosis itself is associated with splenic aneurysm regardless of varix or splenomegaly. *Methods:* In the present study, we retrospectively analyzed 303 cirrhotic patients examined with arteriography. The diagnosis and characteristics of SAAs were determined, and the relation with splenic artery diameter was evaluated. *Results:* Nine patients (2.97%) had 12 complicated SAAs. The aneurysms, which measured 4–22 mm in diameter, were all saccular, and occurred commonly in the splenic hilum (50.0%). A correlation was noted between splenic artery diameter and aneurysm diameter ($R^2 = 0.706$). Aneurysm growth was strongly associated with an increase in diameter of the splenic artery trunk ($R^2 = 0.705$), which is closely related to arterial flow. *Conclusions:* SAA is considered a complication of cirrhosis. The increase in splenic artery diameter may result in SAA enlargement and rupture. Elective procedures should be considered based on the follow-up of main trunk or diameter of the splenic artery in addition to SAA size, a known risk factor of aneurysmal rupture.

Hajime Sunagozaka[1], Hirokazu Tsuji[1,2], Eishiro Mizukoshi[1], Kuniaki Arai[1], Takashi Kagaya[1], Tatsuya Yamashita[1], Akito Sakai[1], Yasunari Nakamoto[1], Masao Honda[1] and Shuichi Kaneko[1]

[1]Department of Gastroenterology, Graduate School of Medical Science, Kanazawa University, Ishikawa, Japan, [2]Department of Gastroenterology, Kanazawa Municipal Hospital, Ishikawa, Japan

Key words: arteriography – liver cirrhosis – rupture – splenic aneurysm – splenic artery diameter

Shuichi Kaneko, Department of Gastroenterology, Graduate School of Medical Science, Kanazawa University, 13-1 Takara-machi, Kanazawa, Ishikawa 920-8641, Japan.
Tel: +81-76-265-2235
Fax: 81-76-234-4250
e-mail: skaneko@medf.m.kanazawa-u.ac.jp

Received 27 March 2005,
accepted 29 November 2005

Splenic artery aneurysm (SAA) is a disease that is usually asymptomatic but has a risk of rupture (1), and can be fatal because of hemorrhagic shock once it ruptures. As its first report in 1770 by Beaussier (2), SAA was thought to be a rare disease. However, recent advances in diagnostic imaging, such as celiac arteriography, Doppler ultrasound examination, and computed tomography (CT) scanning, have increased the chance of diagnosis (3). It has been reported that although the actual incidence of splenic aneurysm in autopsy cases is 0.05–1.6% (4), and it affects 7.1–50% of patients with portal hypertension, which is one of the risk factors in its development (3, 5, 6).

In patients with overt portal hypertension with varices, attention should be paid to the possibility of complication with SAA. However, not all cirrhotic patients have portal hypertensive features, such as gastro-esophageal varices or splenomegaly (7–9), and there have been no large-scale clinical studies of whether cirrhosis itself is associated with SAA even if it is not a complication of portal hypertension. One cirrhotic patient in the present study with no varices actually suffered splenic aneurysmal rupture and died. The SAA development in chronic liver disease should be investigated in terms of the increasing incidence of liver cirrhosis worldwide. Therefore, we conducted a large-scale retrospective clinical study to determine the prevalence of SAA, the incidence of rupture, and its risk factors. In addition, we report the results of examinations along with the follow-up of some patients based on serial arteriography.

Patients and methods

Of the cirrhotic patients admitted to our hospital from January 1996 to May 2004, 303 consecutive patients underwent abdominal arteriography as part of a work up for hepatocellular carcinoma.

In the present study, the images of arteriography were reevaluated retrospectively to detect SAA. Informed consent for arteriography was obtained from each patient and the study protocol conformed to the ethical guidelines of the 1975 Declaration of Helsinki.

Cirrhosis was diagnosed histologically by liver biopsy in almost all patients, but was diagnosed clinically based on liver function tests and imaging findings if patients presented with potential contraindications for percutaneous liver biopsy, such as massive ascites or severe thrombocytopenia. Portal hypertension was estimated from the presence of varices, port-systemic shunts, or splenomegaly. The grade of esophageal varices (grades F0–3) was evaluated according to the classification described previously (10, 11). Splenic aneurysm was diagnosed with celiac arteriography. In patients complicated with SAA, the shape, location, and long diameter of aneurysms, and the maximum diameter of the main trunk of the splenic artery were evaluated. The locations of SAAs were defined as follows: intrasplenic area, splenic hilum, and dividing the main branch of the splenic artery into three equal parts (from the side of the celiac artery), the proximal area, the intermediate area, and the distal area of the splenic artery (12). Six patients with SAAs were examined by multiple arteriographies for 16–37 months (median 25.9). Therefore, the growth rate of SAA could be evaluated with regard to splenic artery diameter.

The possible associations were also investigated between SAA complication and patient characteristics, such as age, gender, cause of cirrhosis, medical history, varices, and splenomegaly. The hepatic reserve and liver fibrosis were assessed from the Child–Pugh score, platelet count, prothrombin time, albumin level, type IV collagen (latex coagulation method), and indocyanine green clearance (ICG15R). The diagnosis and degree of splenomegaly were estimated by the spleen index (SI: the product of the long axis multiplied by the short axis of the spleen, measured from the splenic hilum) based on abdominal ultrasound (Table 1).

The patient who died of hemorrhagic shock following splenic aneurysmal rupture was autopsied. Slides were prepared from tissue samples, which were fixed in 10% buffered formalin, and then examined with hematoxylin–eosin, Elastic van Gieson, and silver staining.

The data are given as means ± standard deviation. The differences in patient characteristics between the SAA and non-SAA (control) groups were tested by the chi-square test, Mann–Whitney *U*-test, and two test.

Results

Incidence of splenic arterial aneurysm

The cirrhotic patients ($n = 303$) consisted of 208 men and 95 women, and had a mean age of 66.3 ± 7.4 years. The cause of cirrhosis was viral hepatitis, particularly hepatitis C virus (HCV), in approximately 75% of the patients. The results of liver function tests were consistent with cirrhosis:

Table 1. Clinical features of patients

	Control group	SAA group
Number	294	9
Age (years)	66.5 ± 7.3	64.3 ± 11.1
Sex (male:female)	205:89	3:6
Etiology		
HBV	45	1
HCV	208	7
HBV+HCV	4	0
Alcohol	24	1
HCV+alcohol	3	0
PBC	10	0
Hematologic characteristics		
Platelet ($\times 10^3/\mu l$)	97.7 ± 48.9	101.0 ± 50.1
Prothrombin time (%)	65.0 ± 16.4	61.2 ± 12.4
Albumin (g/dl)	3.7 ± 0.7	3.7 ± 0.7
Type IV collagen (ng/ml)	270.1 ± 144.9	269.4 ± 160.1
ICGI5R (%)	26.0 ± 14.2 (n = 261)	28.4 ± 13.9 ($n = 7$)
Spelenoindex (cm^2)	29.2 ± 14.1(n = 228)	25.8 ± 9.4
Child–Pugh score	6.5 ± 1.3	6.2 ± 1.1
Complicated varix	54.4% (160/294)	44.4%(4/9)

Data are given as mean ± SD, there are no data with $P < 0.05$. SAA, splenic artery aneurysm; HBV, hepatitis B virus; HCV, hepatitis C virus; PBC, primary biliary cirrhosis.

decreases in platelet count, prothrombin time result, and albumin level; increases in ICG15R value and type IV collagen; and varices (Table 1).

Nine of all the patients were complicated with SAA, and had an average age of 64.3 ± 11.1 years at the time of diagnosis, which was not significantly different from the non-complicated patients. The Child–Pugh score for the nine patients with SAA averaged 6.2 ± 1.1. Of the nine patients with SAA, three were men and six were women, indicating sex-specific difference ($P = 0.020$). Two of the six women had a history of three or more pregnancies. Hepatitis B virus, HCV, and alcoholic liver disease caused cirrhosis in one, seven and one of the patients with SAA, respectively. There were no significant differences in platelet count, prothrombin test result, albumin level, type IV collagen level, ICG15R value, esophageal varices, or SI between the patients with and without SAA (Table 1).

Characteristics of splenic artery aneurysm

Nine patients had a total of 12 SAAs, which were not complicated by calcification or thrombi. Multiple SAAs (up to three) were observed in two patients. The SAAs ranged in diameter from 4 to 22 mm (mean 14.1 mm), and were saccular regardless of size or location. No fusiform SAA was observed. One SAA was located in each of the proximal (8.3%), intermediate (8.3%), and distal (8.3%) segments; six SAAs (50.0%) in the splenic hilum; and three SAAs (25.0%) within the spleen (Table 2). One hundred and sixty (54.4%) of the 294 patients without SAA, and four (44.4%) of the nine patients with SAA were complicated with esophageal varices. Moreover, 171 (58.1%) of the 294 patients without SAA, and eight (88.9%) of the nine patients with SAA were complicated with splenomegaly. However, there were no significant differences in the degree of SI between the patients with and without SAA ($P = 0.781$) (Table 1).

Splenic artery aneurysm and splenic artery

The splenic hyperkinetic state is associated with the development of SAA (5, 6, 13–16). As shown in Fig. 1, we observed a correlation between the diameter of the main trunk of the splenic artery and the size of complicating SAA ($R^2 = 0.706$). In addition, we confirmed the serial changes in eight SAAs occurring over long periods in six patients by celiac arteriography, which was performed to examine hepatocellular carcinoma. During the 16–37 months of follow-up (median 25.9), the diameter of the main trunk of the splenic artery and the long diameter of the SAAs increased by 0.18 and 2.65 mm on average, respectively (Fig. 2). Time-lapse observations indicated that the SAA diameter remained unchanged in some patients, but increased in others, such as Case No. 5 shown in Fig. 3. The increase in main trunk of the splenic artery rather than the main trunk diameter itself, contributed to the increase in SAA diameter ($R^2 = 0.705$) (Fig. 4).

Analysis of ruptured SAA

One patient with SAA (Case No. 1) died of hemorrhagic shock because of rupture (Table 2). Autopsy revealed an irregular internal elastic lamina of the ruptured aneurysm wall with vacuolar degeneration and thinning of the tunica media. As the defects of the intima, tunica media, and adventitia corresponded to a massive subserosal hematoma, the cause of death was diagnosed as SAA rupture. Another noteworthy lesion was an organized thrombus that was located in the splenic vein and extended to the main trunk of the

Table 2. Clinical features of patients with splenic aneurysm

Case no.	Age	Sex	Etiology	Splenic aneurysm			Main trunk of splenic artery (mm)	Splenoindex (cm^2)	Esophageal varix	Remark
				Number	Location	Size (mm)				
1	55	M	HCV	2	H	22.0	8.4	7.6 × 6.2	(–)	Ruptured
					M	10.0				
2	71	F	HCV	1	I	4.6	3.8	4.9 × 4.5	(–)	
3	80	M	Alcohol	1	H	12.0	5.0	5.1 × 4.7	F1	
4	62	F	HCV	1	I	6.0	5.0	5.5 × 4.5	(–)	
5	63	F	HCV	1	H	18.0	4.8	5.5 × 4.6	F2	3 pregnancies
6	73	F	HCV	3	H	22.0	5.0	4.9 × 4.9	F1	
					P	20.0				
					D	15.0				
7	44	F	HCV	1	H	18.0	6.0	5.7 × 5.1	(–)	4 pregnancies
8	58	M	HCV	1	I	4.0	4.0	6.0 × 4.2	F0	
9	73	F	HBV	1	H	15.0	5.8	3.6 × 3.0	(–)	

Location: P, proximal; M, intermediate; D, distal; H, hilus; I, intrasplenic; M, male; F, female; HCV, hepatitis C virus; HBV, hepatitis B virus.

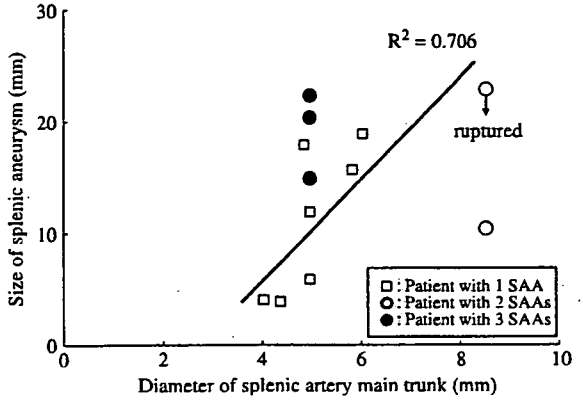

Fig. 1. Correlation between splenic artery diameter and size of splenic artery aneurysm (SAA). Open and closed circles represented the patients with two and three SAAs, respectively. Open squares represented the patients with one SAA. We observed a correlation between the diameter of the main trunk of the splenic artery and the size of complicating SAA ($R^2 = 0.706$).

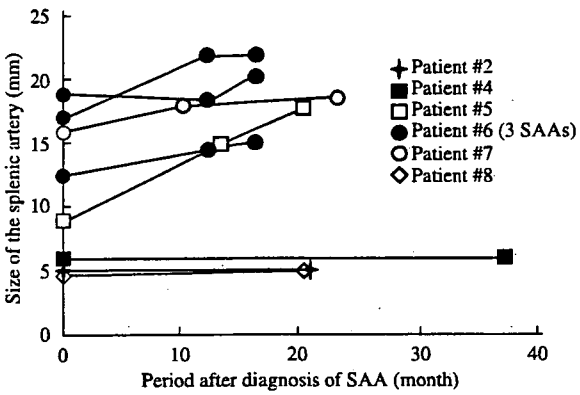

Fig. 2. Sequential changes of splenic artery aneurysms (SAAs). The sizes of eight SAAs in six patients were measured sequentially by celiac arteriography during a mean follow-up period of 25.9 months. The diameter of the main trunk of the splenic artery and the long diameter of the SAAs increased by 0.18 and 2.65 mm on an average, respectively. Note that some SAAs became enlarged, while the sizes of others remained unchanged.

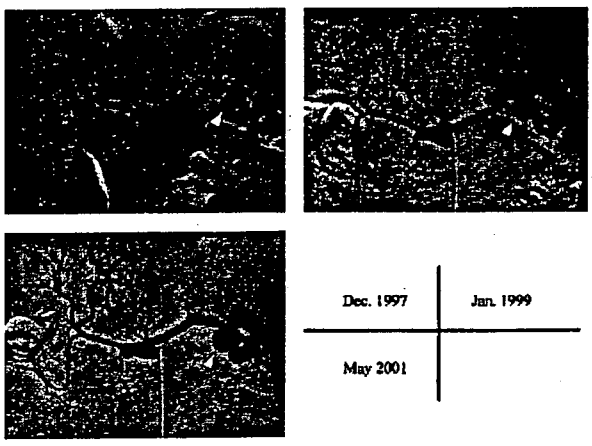

Fig. 3. Sequential changes of splenic artery aneurysm (SAA) on celiac arteriography. Arrowheads indicate the SAA, and its diameter was shown to have increased (Case No. 5).

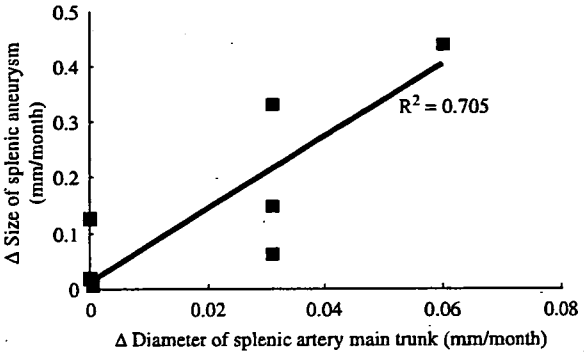

Fig. 4. Correlations between the growth rate of splenic artery diameter and size of splenic artery aneurysm. The tendency of the main trunk of the splenic artery to increase, that is, the tendency of splenic blood flow to increase contributed to the elevation in the splenic aneurysm diameter.

portal vein, but had not been detected by imaging 4 months before death (Fig. 5).

Discussion

SAA clinical presentation and characteristics in liver cirrhosis

The incidence of SAA varies widely depending on the subjects studied, and has been reported to be 0.05–1.6% in general autopsies (4). Multiple risk factors for the formation of SAAs have been reported (17, 18), and the high-risk group should be followed up carefully or given preventive therapy because SAA rupture is associated with a high mortality rate. The actual incidence of SAA in portal hypertensive patients diagnosed by the presence of esophageal and gastric varices has been reported to be 7.1–50% (3, 5, 6, 13, 16, 19), which is higher than that in the general population. However, previous studies were designed to detect only patients with varices. Although varices are a frequent sign of portal hypertension, the prevalence is only 44–51% (20, 21). Moreover, patients without varices, such as Case No. 1, could present aneurysmal rupture, suggesting that hemodynamics in liver cirrhosis should be considered risk factors of rupture. The present study was the first to analyze SAA in cirrhotic patients regardless of portal hypertensive signs, such as varices. With recent advances in technology, celiac arteriography is now used to examine hepatocellular carcinoma in cirrhotic patients to predict the stage of disease and to determine treatment management (22, 23). Angiography remains the gold standard to localize the lesions and determine the presence of SAA (24), and retrospective estimation of arteriography can allow the detection of incidental splenic aneurysm.

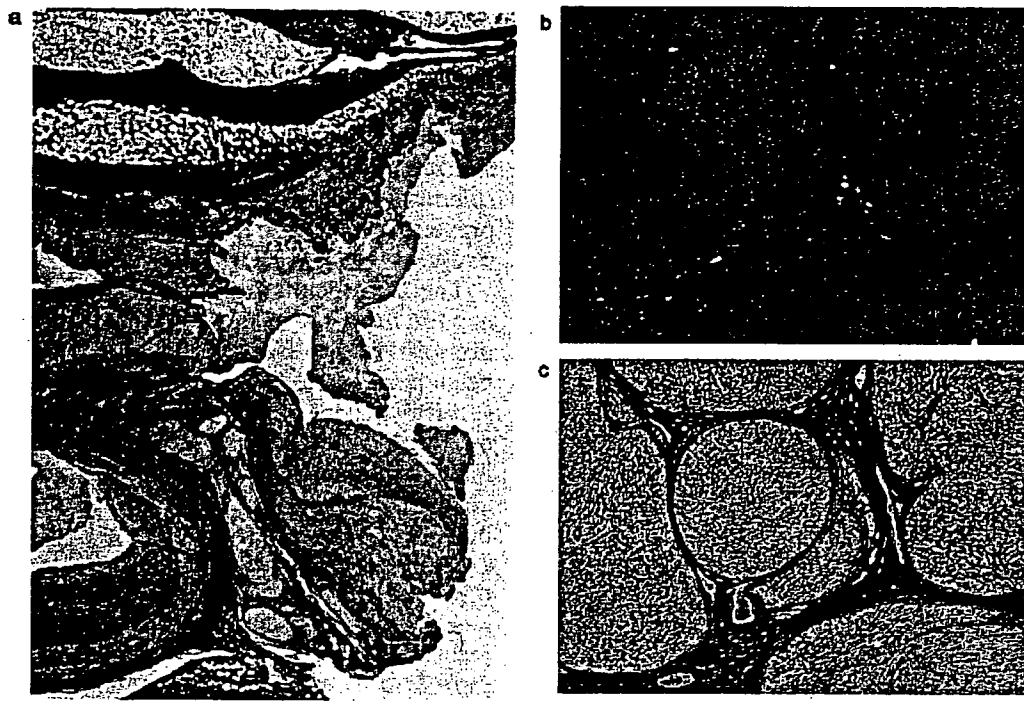

Fig. 5. Histopathological examination of ruptured aneurysm and cirrhotic liver tissue. (a) The ruptured aneurysm showing an irregular internal elastic lamina and vacuolar degeneration and thinning of the tunica media. The defects of the intima, tunica media, and adventitia corresponded with a massive subserosal hematoma (arrow). (Elastic van Gieson stain, × 4). (b, c) The hepatic parenchyma dysplayed fibrosis and nodule formation of varying sizes, implying liver cirrhosis. (b) Hematoxylin–eosin stain, × 32; (c) Silver stain, × 32).

In the present study, complicating gastroesophageal varices and splenomegaly (SI > 20) were observed in 54.1% (164/303) and 59.1% (179/303) of the cirrhotic patients analyzed, respectively, i.e., in about half of the patients. Nine (2.97%) of the 303 cirrhotic patients had SAA. All nine cases were diagnosed histologically as liver cirrhosis. Four of 164 patients with varices (2.4%) and five of the 139 patients without varices (3.6%) had SAA. Thus, we could not determine the risk of SAA based solely on the presence of varices. Moreover, the size of the spleen (SI) in SAA patients was not significantly different from that in the non-SAA patients ($P = 0.781$). Although the incidence of SAA in the present study was lower than that in patients with varices reported previously (3, 5, 6, 25), it was about 1.9–59.4-fold higher than the incidence reported in autopsy cases where no patient characteristics were defined (4). The lower prevalence may have been because angiography was only used to examine patients with at least one episode of varix bleeding or advances in image analysis allowed us to distinguish early cirrhosis from chronic hepatitis although liver cirrhosis was finally diagnosed by liver biopsy. These findings suggested a need to regard not only varices but also cirrhosis itself as associated factors for SAA. Cirrhotic patients undergoing arteriography should be evaluated for not only intrahepatic malignancy (22, 23) but also for SAA.

Mechanism for development of SAA

In the present study, we evaluated the location, size, and changes in size of SAAs accurately by serial arteriography. The ruptured aneurysm in the present study measured 22 mm. A previous report suggested that the risk of rupture might be linked to size (18), which is associated with splenic artery flow (6, 13). Arterial blood flow has been clearly shown to be related to arterial diameter (26). The question arises whether the size of SAA is correlated with the diameter of the splenic artery. In the present study, we found a relationship between SAA diameter and the main trunk of the splenic arteries as shown in Fig. 1. Cirrhosis-associated changes in hemodynamics systemically result in increased cardiac output, increased vascular contents, and portal congestion with outflow impairment. Then, the hemodynamic changes impose stress on the vascular wall of the portal vein with resultant primary alterations in wall structure, leading to local vascular dilation and splenic aneurysm formation (5, 14–16, 27). We consider that in the splenic

artery, the increase in splenic artery blood flow is closely related to the growth of SAA.

In addition, we have followed SAAs over long periods by abdominal arteriography, and our results have indicated that some SAAs became enlarged, while others did not change in size, as shown in Fig. 2. The most rapid growth rate was 9 mm over 20 months. Notably, not a longer follow-up period but an increase in the diameter of the splenic artery was associated with faster enlargement of SAAs. The increase in splenic artery diameter was also thought to be essential for the growth of the SAA.

Risk of rupture and management of SAA

SAA rupture is accompanied by massive intraperitoneal hemorrhage leading rapidly to hemorrhagic shock and poor prognosis. Boijsen and Efsing (13) and Spittel et al. (28) reported rupture frequencies of 6% and 8.2%, respectively. Berger et al. (29) reported that the frequency of rupture secondary to portal hypertension was 35%. Although hemostatic procedures, such as open abdominal splenic aneurysm ligation and splenectomy, and transcatheter embolization are indicated for the treatment of splenic aneurismal rupture (30–32), the prognosis remains poor. Lee et al. (19) reported a mortality rate of 17% after SAA rupture in patients with no portal hypertension complication, whereas portal hypertensive patients had a significantly poorer prognosis with a mortality rate of 57%. They also reported that 84% of patients undergoing elective procedures survived after a mean follow-up period of 46 months. Therefore, identification of risk factors for SAA rupture and appropriate preventive measures are more important than treatment after rupture.

Risk factors for rupture included no encapsulation (calcification), aneurysm size, and a tendency toward enlargement, clinical symptoms, and pregnancy (17). It has been reported that aneurysms less than 15 mm in diameter have a low risk of rupture, making them amenable to conservative follow-up (33), whereas about 3–10% of aneurysms more than 20 mm in diameter rupture (3, 13, 17, 34). In the present study, two patients had a total of three aneurysms more than 20 mm in maximum long diameter, one of which ruptured. None of the five aneurysms less than 15 mm in diameter ruptured. Although the size of SAA is a significant risk factor, the splenic artery flow related to the diameter of the splenic artery should be measured to estimate the risk. The patient who died of rupture in the present study had portal thrombosis, which was confirmed at autopsy but had not been diagnosed by imaging 4 months before death. We speculate that rapid thrombus formation resulted in a rapid increase in splenic artery pressure secondary to stagnation of blood flow in the spleen, leading to growth and rupture of the fragile aneurysm. In cases in which splenic flow is increasing, it is necessary to take preventive procedures and to treat them aggressively.

The treatment option is limited by impaired hepatic function. Although open combined resection of the splenic artery and spleen has generally been performed (19), less-invasive laparoscopic surgical procedures are now possible depending on the location and number of SAAs (35, 36). Partial splenic embolization could be used as an alternative procedure dependent on our study because it decreases splenic flow (37) resulting in prevention of aneurysmal rupture. To determine the indication for treatment, celiac arteriography has the highest sensitivity for the diagnosis and measurement of SAA (31). However, this procedure is too invasive for follow-up. Therefore, a few studies have reported that less-invasive Doppler ultrasound was useful for assessment of the size of SAAs and the amount of splenic arterial blood flow (27, 38). Elective measures could be considered in patients with SAA if increase in aneurysmal size or splenic artery diameter are observed.

Conclusions

The incidence of SAA in cirrhotic patients is 2.97%, and about 1.9-59.4-hold higher than that of the general population. The increase in main trunk of the splenic artery, i.e., the increase of splenic blood flow, rather than the main trunk diameter itself, contributed to the increase in SAA diameter. SAA is considered to be a complication of cirrhosis. Increases in splenic artery diameter contribute to the progression and rupture of the SAA. Elective procedures should be considered for high-risk groups.

References

1. Stanley J C, Wakefield T W, Graham L M, Whitehouse W M Jr., Zelenock G B, Lindenauer S M. Clinical importance and management of splanchnic artery aneurysms. J Vasc Surg 1986; 3: 836–40.
2. Beaussier M. Sur un anevrisme de l'artere splenique: dont les parois se sont ossifiees. J Med Clin Pharmacol Paris 1770; 32: 157.
3. Stanley J C, Fry W J. Pathogenesis and clinical significance of splenic artery aneurysms. Surgery 1974; 76: 898–909.
4. Moore S W, Guida P M, Schumacher H W. Splenic artery aneurysm. Bull Soc Int Chir 1970; 29: 210–8.